International Journal of Minerals, Metallurgy and Materials
Volume 24, Number 3, March 2017, Page 316
DOI: 10.1007/s12613-017-1410-9

Effect of Fe_2O_3 on the crystallization behavior of glass-ceramics produced from naturally cooled yellow phosphorus furnace slag

Hong-pan Liu[1)], *Xiao-feng Huang*[1)], *Li-ping Ma*[1)], *Dan-li Chen*[1)], *Zhi-biao Shang*[1)], *and Ming Jiang*[1,2)]

1) Faculty of Environmental Science and Engineering, Kunming University of Science and Technology, Kunming 650500, China
2) College of Resources and Environment, Yunnan Agricultural University, Kunming 650201, China
(Received: 29 August 2016; revised: 27 October 2016; accepted: 31 October 2016)

Abstract: $CaO–Al_2O_3–SiO_2$ (CAS) glass-ceramics were prepared via a melting method using naturally cooled yellow phosphorus furnace slag as the main raw material. The effects of the addition of Fe_2O_3 on the crystallization behavior and properties of the prepared glass-ceramics were studied by differential thermal analysis, X-ray diffraction, and scanning electron microscopy. The crystallization activation energy was calculated using the modified Johnson–Mehl–Avrami equation. The results show that the intrinsic nucleating agent in the yellow phosphorus furnace slag could effectively promote the crystallization of CAS. The crystallization activation energy first increased and then decreased with increasing amount of added Fe_2O_3. At 4wt% of added Fe_2O_3, the crystallization activation energy reached a maximum of 676.374 $kJ·mol^{-1}$. The type of the main crystalline phase did not change with the amount of added Fe_2O_3. The primary and secondary crystalline phases were identified as wollastonite ($CaSiO_3$) and hedenbergite ($CaFe(Si_2O_6)$), respectively.

Keywords: glass-ceramics; nucleation; crystallization; activation energy; iron oxides

1. Introduction

Yellow phosphorus furnace slag is a solid byproduct generated during the production of phosphorus. Phosphorus can be produced from natural phosphorus ore via either the electric furnace or the blast furnace process, and different heating methods and raw materials can be used. In both processes, silica is added as a flux and coke as a reducing agent before the ore is heated to 1350–1400°C, where the phosphorus evaporates. The phosphorus is then obtained through condensation in a refining system. According to the cooling method, the yellow phosphorus furnace slag can be divided into water-quenched slag and the naturally cooled state of yellow phosphorus furnace slag. In the water quenching process, the molten yellow phosphorus furnace slag is rapidly cooled from a high temperature to room temperature using water. In this case, the cooling time is sufficiently short to prevent a new phase from forming in the internal slag. By contrast, in case of the natural cooling treatment, the molten furnace slag is allowed to cool in air. Here the cooling rate is low and a new phase can form in the interior of the slag.

In recent years, several groups have studied the utilization of phosphorus furnace slag, e.g., for the preparation of silica [1], ceramic materials [2], agricultural calcium fertilizer [3], glass materials [4], and glass-ceramics [5]. Using phosphorus furnace slag for the production of high value-added glass-ceramics appears to be a particularly effective method to ensure a more comprehensive utilization.

Glass-ceramics are fine-grained polycrystalline materials synthesized by carefully controlling both the composition of the slag [6] and the heat-treatment conditions [7]. These materials are inexpensive and exhibit low water absorption, high acid resistance, and excellent mechanical properties. The major constituents of yellow phosphorus furnace slag are CaO and SiO_2; however, the slag also contains numerous oxides, such as Al_2O_3, TiO_2, Fe_2O_3, P_2O_5, MgO, K_2O, and Na_2O. Depending on the composition of the yellow phosphorus furnace slag, it might be suitable as a new raw material for the preparation of glass-ceramics. Various metallurgical slags, including blast furnace slag [8–10], copper slag [6,11], ferrous tailing slag [12], and sludge [13], have

Corresponding author: Xiao-feng Huang E-mail: hxfkmust@163.com

been studied for the preparation of glass-ceramics. Recent studies have shown that TiO_2, Fe_2O_3, Cr_2O_3, and CaF_2 [14–16] are effective crystallization agents. For instance, Alizadeh *et al.* [17] introduced Fe_2O_3 as an effective nucleating agent into the MgO–CaO–SiO_2 P_2O_5 system. They noted that the addition of 5.0wt% Fe_2O_3 to the glass resulted in a high relative density and good mechanical strength of the prepared glass-ceramic material. Wang [18] found that the addition of a certain amount of iron oxide (approximately 4.2wt%) into the MgO–Al_2O_3–SiO_2 glass-ceramic system was beneficial to the crystallization process. Wang *et al.* [19] reported that the iron-rich system exhibited lower melting, glass-transition, and glass-crystallization temperatures. Yang *et al.* [20] investigated the effect of Fe^{2+} and Fe^{3+} ions on the crystallization behavior of CaO–Al_2O_3–SiO_2–MgO glass-ceramics, and their results indicated that the addition of Fe^{2+} decreased the crystallization temperature, whereas the addition of Fe^{3+} ions as the nucleating agent improved the crystallization behavior. Thus, a survey of the related literature suggests that most researchers have focused on the sintering process of the glass-ceramics and the effect of Fe_2O_3 as a nucleating agent on the crystallization of slag or fly ash. By contrast, a melting process has thus far not been used to produce glass-ceramics prepared from naturally cooled yellow phosphorus furnace slag, and the effect of the Fe_2O_3 nucleating agent in the slag on the crystallization process is not clear.

Therefore, the aim of this work was to investigate the effect of the addition of an extra amount of Fe_2O_3 as the nucleating agent on the crystallization behavior of the CaO–Al_2O_3–SiO_2 (CAS) glass-ceramic system and to develop sufficient theoretical understanding to enable selection of an appropriate nucleating agent for glass-ceramics prepared from a naturally cooled yellow phosphorus furnace slag. Furthermore, the effects of the addition of Fe_2O_3 as a nucleating agent on the crystallization kinetics, phase composition, and properties of the prepared CAS glass-ceramics were investigated in this study.

2. Experimental

The naturally cooled yellow phosphorus furnace slag (from Yunnan Province, China) was ground and sieved to the number of 180 meshes. The slag was dried at 105°C for 24 h, and then mixed with SiO_2, Al_2O_3, and Fe_2O_3. The powder mixture was heated at 1350°C for 2 h in an electric furnace. To minimize internal stress, the as-cast and the treated samples of the parent glass were first annealed at 600°C for 2 h and then naturally cooled to room temperature. Table 1 shows the chemical composition of the naturally cooled yellow phosphorus furnace slag, as analyzed by X-ray fluorescence (XRF) spectrometry. As shown in Table 1, the main components of the yellow phosphorus furnace slag were CaO and SiO_2.

Table 1. Composition of naturally cooled yellow phosphorus furnace slag from a chemical phosphorus plant in Yunnan Province, China wt%

CaO	SiO_2	Al_2O_3	MgO	P_2O_5	F	Fe_2O_3	Na_2O	K_2O	Others
47.98	30.45	2.89	5.35	3.79	2.93	0.059	0.21	0.37	5.971

The phase composition of the slag was investigated by X-ray diffraction (XRD, D/max-2200) using Cu K_α radiation. The patterns were recorded over the 2θ range from 10° to 80° at a scanning rate of 0.02 min^{-1}, and the diffractometer was operated at 36 kV and 30 mA. The main crystal phases of the naturally cooled yellow phosphorus furnace slag were confirmed using the Jade 5.0 software. Fig. 1 shows that gehlenite ($Ca_2Al_2SiO_7$, JCPDF No. 35-0755), fluorapatite ($Ca_5(PO_4)_3$, JCPDF No. 15-0876)), and wollastonite ($CaSiO_3$, JCPDF No. 02-0506) were the main crystalline phases of the samples. To investigate the influence of the addition of Fe_2O_3 as a nucleation agent, the as-received Fe_2O_3 was added to the naturally cooled yellow phosphorus furnace slag. Table 2 shows the composition of

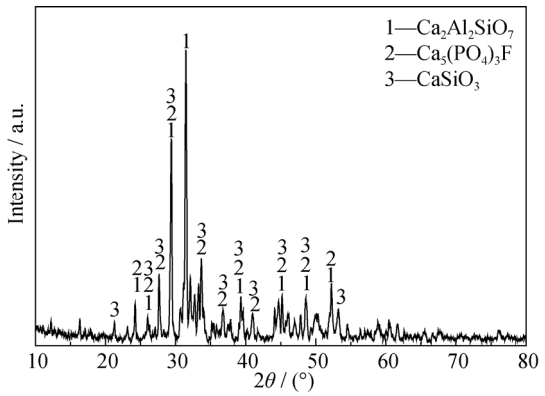

Fig. 1. XRD pattern of the naturally cooled yellow phosphorus furnace slag.

the CAS glass-ceramic. ZL represents the sample in which no as-received Fe_2O_3 was added into the naturally cooled yellow phosphorus furnace slag. ZLFe2 represents the sample in which 2wt% Fe_2O_3 was added into sample ZL, ZLFe4 represents the sample in which 4wt% Fe_2O_3 was added, and ZLFe6 represents the sample in which 6wt% Fe_2O_3 was added.

Table 2. Composition of the CAS glass-ceramic wt%

Sample	Slag	SiO_2	Al_2O_3
ZL	63.4	33.8	2.8

Differential thermal analysis (DTA) was performed on a differential thermal analyzer (SHIMADZU DTG-60H) at different heating rates ranging from 5 to 20°C·min^{-1} to study the thermal behavior of the CAS glass. An empty crucible was used as reference. The phase composition of the prepared glass-ceramics were again investigated by XRD in the 2θ range from 5° to 90° at a scanning rate of 3°·min^{-1}. Scanning electron microscopy (SEM, VEGA3) was used to observe the microstructure of the prepared glass-ceramic samples after they were etched for 30 s in 1.5vol% HF and then dried at 105°C. The acid resistance was evaluated by the mass loss percentage: $(m_0 - m_1)/m_0 \times 100\%$, where m_0 and m_1 were the mass of the samples before and after corrosion, respectively. The bulk density was determined using the Archimedes principle. The water absorption and acid and alkaline resistance of the samples were analyzed according to the JC/T872—2000 building material industry standard.

3. Results and discussion

3.1. Kinetics analysis

A certain amount of energy was required for the glass to overcome the phase and structure unit rearrangement barrier to transform into a crystalline structure during the crystallization process, i.e., the activation energy for crystallization. To investigate the crystallization kinetics, the values of the activation energy (E), the frequency factor (v), and the crystallization rate constant (k) were calculated for the different non-isothermal methods. These parameters can provide an important theoretical basis for estimating the crystallization activation energy.

Fig. 2 shows the DTA curves obtained for the different samples at different heating rates, i.e., 5, 10, and 15°C·min^{-1}.

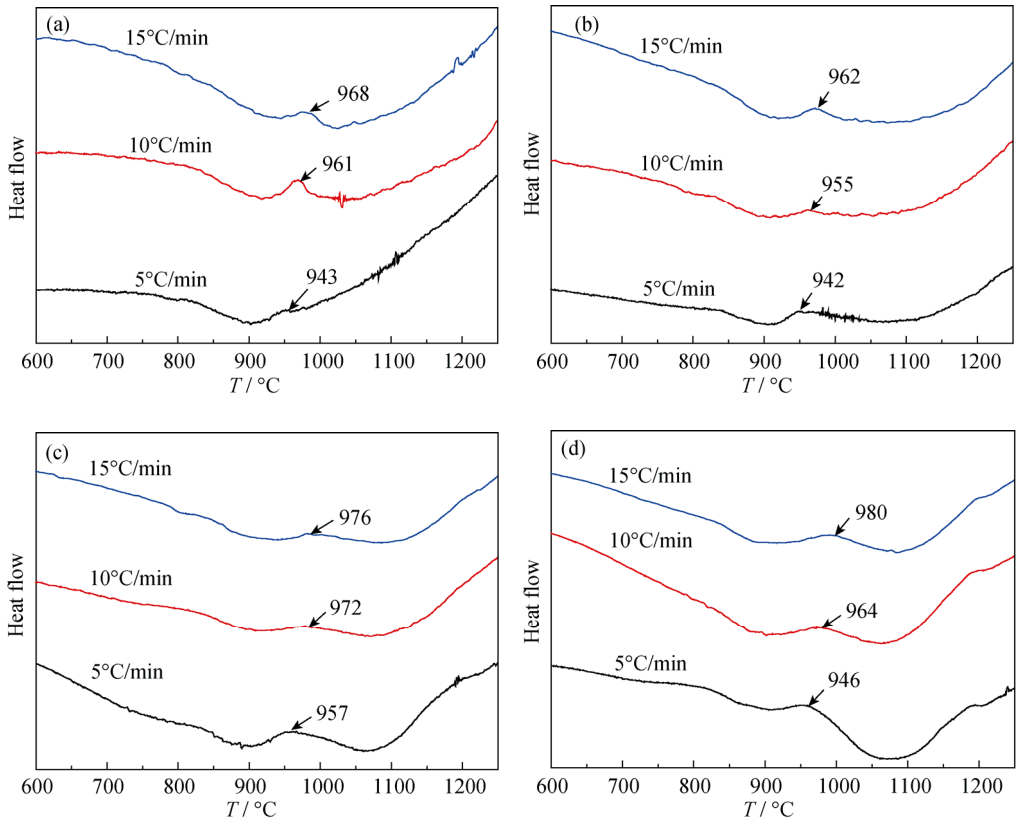

Fig. 2. DTA curves of the CAS glass-ceramic system: (a) ZL; (b) ZLFe2; (c) ZLFe4; (d) ZLFe6.

These DTA curves indicate that the local maximum associated with the crystallization temperature (T_p) shifted to a higher value as the heating rate was increased. The activation energy for crystallization of the parent glass samples was estimated from the DTA curves. The modified Johnson–Mehl–Avrami (JMA) equation [21–22] was used to describe the glass crystallization ability according to the DTA data:

$$x = 1 - \exp[-(kt)^n],$$

where x is the transformed phase volume fraction, n is the crystal growth index, and k is the crystallization rate constant. The crystallization rate constant k is calculated through the Arrhenius equation:

$$k = v \cdot \exp\left(-\frac{E}{RT}\right),$$

where R is the gas constant and T is the absolute temperature. According to Kissinger [23–24], E can be obtained as

$$\ln\frac{T_p^2}{\beta} = \frac{E}{R\,T_p} + \ln\frac{E}{R\,v},$$

where β is the heating rate.

According to the results presented in Table 3, the crystallization activation energy of the CAS glass-ceramic system increased with increasing amount of added Fe_2O_3. When the amount of added Fe_2O_3 reached 6wt%, the crystallization activation energy decreased. A decrease in the general E value was preferred to enhance the crystallization of the glass.

Table 3. Kinetic parameters of CAS glass-ceramics containing Fe_2O_3 nucleating agent

Sample	Activation energy, E / (kJ·mol^{-1})	Frequency factor, v	Crystallization rate constant, k
ZL	516.5961	3.19×10^{21}	3.03×10^{21}
ZLFe2	661.8502	7.62×10^{27}	3.99×10^{27}
ZLFe4	676.3740	1.39×10^{28}	1.30×10^{28}
ZLFe6	391.6751	9.94×10^{15}	9.57×10^{15}

Fig. 3 shows plots of $\ln\frac{T_p^2}{\beta}$ vs. $\frac{1}{T_p}$, illustrating the variation of the crystallization activation energy with the amount of Fe_2O_3 added as a nucleation agent. The crystallization activation energy first increased and then decreased with increasing amount of added Fe_2O_3. At 4wt%, the crystallization activation energy reached a maximum of 676.3740 kJ mol^{-1}. This behavior is explained as follows. The Fe^{3+} ions cause a lattice distortion and increase the energy of the crystal form, thereby increasing the crystallization activation energy [25–26]. However, the Fe^{3+} ions also form [FeO_4] tetrahedra to replace the Si^{4+} tetrahedra, thereby repairing the network structure and increasing the viscosity of the glass, which, in turn, reduces the reaction rate of the Fe^{3+} ions during the crystallization process. Consequentially the crystallization ability and the heat release of the crystalline samples gradually decreased [27]. However, the large number of iron ions in the parent glass can promote glass phase separation and also provide the driving force for the glass core to promote the glass crystallization inside [28].

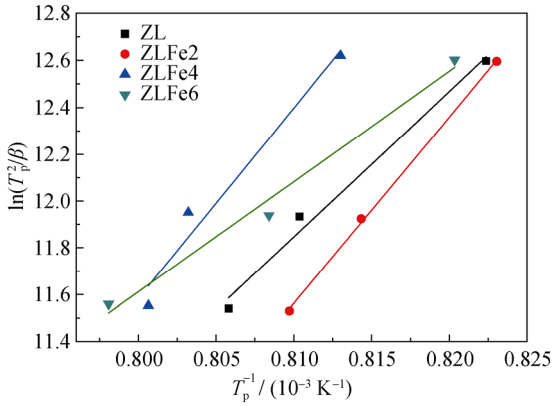

Fig. 3. Diagram of $\ln\frac{T_p^2}{\beta}$ vs. $\frac{1}{T_p}$ for CAS system glass-ceramics.

3.2. Phase analysis

According to the comprehensive XRD profiles, the addition of Fe_2O_3 as a nucleating agent also substantially affected the internal structure of the prepared CAS glass-ceramics. Prior to the XRD analysis, the glass specimens were heated at 790°C for 2 h and then at 1080°C for 1.5 h to obtain the microcrystalline glass. The glass-ceramic powder was ground in an agate mortar. The powder was then analyzed by XRD to determine the phase composition; the results are shown in Fig. 4.

The main crystal phase of each sample was identified by XRD. Fig. 4 shows that all samples mainly consist of wollastonite ($CaSiO_3$) and hedenbergite ($CaFe(Si_2O_6)$). The amount of added Fe_2O_3 was found to weakly influence the phase composition of the CAS system. The peak intensity observed for sample ZL was higher than those measured for the ZLFe series of samples with extra Fe_2O_3, suggesting a higher degree of crystallization in sample ZL. The peak intensity observed for sample ZLFe4 was higher than those obtained for the samples ZLFe2 and ZLFe6. Greater peak intensities indicate a greater degree of crystallization. The

crystallinity and average grain size of the glass-ceramics were assessed using the Scherrer equation, which is widely used to determine the size of crystallite particles in powders. It is written as

$D_{hkl} = K \cdot \lambda / (\beta \cdot \cos\theta)$,

where D_{hkl} is the average grain size of the crystalline domains, K is a dimensionless shape factor with a value of approximately unity (typically ~0.9), λ is the X-ray wavelength (0.15406 nm in this case), β is the full width at half-maximum (FWHM), and θ is the Bragg angle.

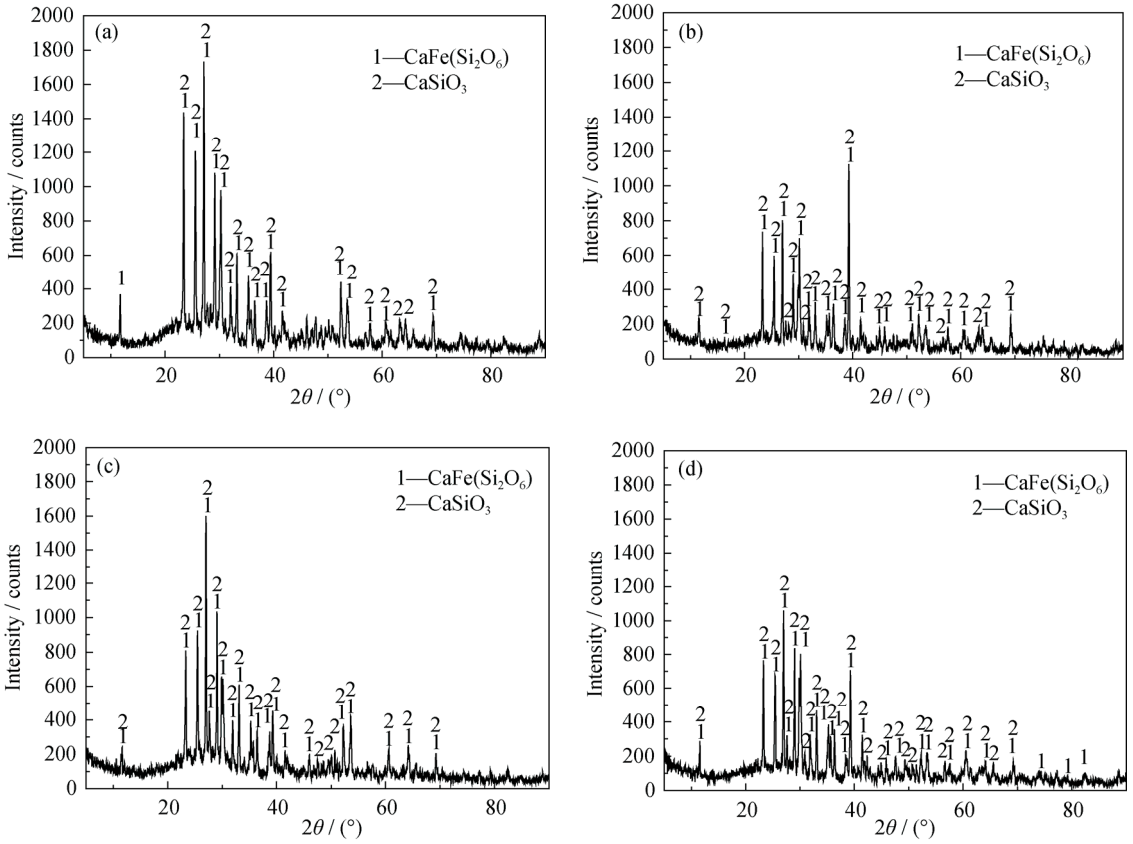

Fig. 4. XRD patterns of glass-ceramics: (a) ZL; (b) ZLFe2; (c) ZLFe4; (d) ZLFe6.

The values obtained for the crystallinity and crystallite size of the CAS glass-ceramics prepared from powders containing various amounts of Fe_2O_3 as a nucleating agent are compared in Fig. 5. The crystallite size was the smallest for sample ZLFe4 at 69.7 nm; sample ZLFe6 exhibited the lowest degree of crystallinity.

3.3. Macroscopic morphology and micrograph analysis

Photographs of the cross-sections of the different samples are shown in Fig. 6. The color of sample ZL was white, and the color changed into yellow when 2wt% of Fe_2O_3 was added to the raw materials. With increasing amount of added Fe_2O_3, the color of the sample gradually changed to gray-green and eventually to black. When the amount of added Fe_2O_3 reached 6wt%, the glass phase began to appear inside the system and the overall crystallization was surface crystallization. Increasing the amount of added Fe_2O_3 inhibited the overall crystallization of the glass-ceramics but enhanced the trend of surface crystallization.

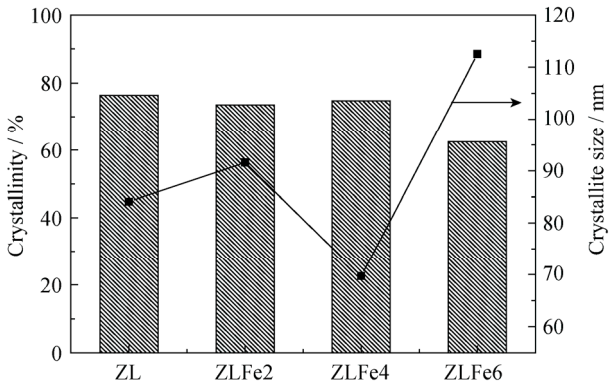

Fig. 5. Crystallinity and crystallite size of glass-ceramics.

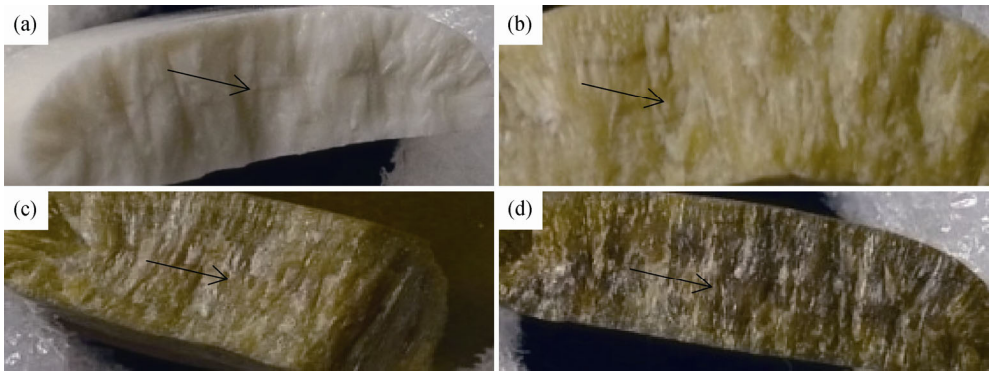

Fig. 6. Photos of the cross sections of samples ZL (a), ZLFe2 (b), ZLFe4 (c), and ZLFe6 (d).

Fig. 7 shows the SEM micrographs of the glass-ceramics after heat treatment. A large number of granules were found in these glass-ceramic samples. The section of sample ZL prepared without the nucleating agent showed the overall crystallization phenomenon illustrated in Fig. 6, and the grains in sample ZL exhibited the globular and short-columnar shape in Fig. 7(a). In the case of sample ZLFe4, the grain size of the internal glass phase was smaller than that obtained for samples ZL and ZLFe2, consistent with the XRD results. When 2wt% of Fe_2O_3 was added, the grain color became yellow (Fig. 6(b)) and the section showed a lamellar crystal distribution. When 6wt% of Fe_2O_3 was added, the specimen exhibited knitting in its interior, accompanied by the appearance of the glass phase in the interior. According to the macroscopic morphology and the micrograph analysis, the CAS system can already crystallize without the nucleating agent and the addition of a small amount of Fe_2O_3 as nucleating agent inhibits the crystallization process. This behavior is explained as follows: Initially, the network modification due to the presence of the Fe^{3+} ions increases the crystallization activation energy; it subsequently decreases when more Fe_2O_3 is added. Thus, the crystallization process was first inhibited when the Fe^{3+} ions were introduced into the system and was eventually enhanced when the concentration of Fe^{3+} ions exceeded a certain threshold level. SEM observations revealed that the crystal grain size decreased when 4wt% of Fe_2O_3 was added; because the space for crystal growth was limited, the grain size decreased.

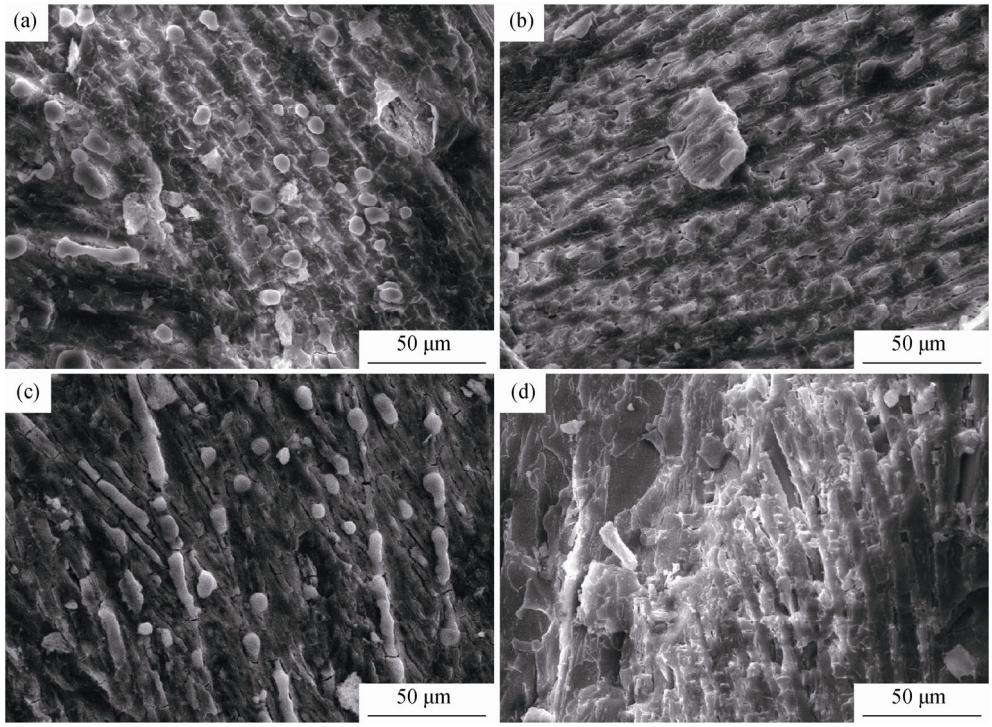

Fig. 7. SEM images of samples ZL (a), ZLFe2 (b), ZLFe4 (c), and ZLFe6 (d).

3.4. Material properties

Material property tests were performed on samples ZL, ZLFe2, ZLFe4, and ZLFe6 according to standard JC/T872-2000 standard. The results are shown in Table 4.

Table 4. Material properties of the glass-ceramics with different Fe_2O_3 contents

Sample	Density / ($g \cdot cm^{-3}$)	Water absorption / wt%	Acid resistance / wt%	Alkali resistance / wt%
ZL	1.9359	0.0147	0.1935	0.0072
ZLFe2	1.9353	0.0120	0.1207	0.0090
ZLFe4	2.2216	0.0029	0.1032	0.0032
ZLFe6	1.7694	0.0075	0.0980	0

The density of the glass-ceramics was found to exhibit the opposite trend as the crystallite size distribution. The additional Fe^{3+} ions enhanced both the acid resistance and the alkali resistance, in agreement with the results published by Singh and Bahadur. [29]. The Fe^{3+} ions can also mend the [Si–O] net structure and increase the chemical durability. The glass density mainly depends on the atomic mass of the glass, the atomic packing factor, and the coordination number [30]. The variation of the chemical composition of the glass-ceramics was found to have little influence on their density. By contrast, the crystallization process itself strongly influenced the density of the glass-ceramics. The density of glass-ceramics mainly depends on the type and quantity of the precipitate phase. The volume shrinkage of the sample and the density increases when a large proportion of crystals with a fine grain size is contained in a small amount of residual glass [31]. In the present work, the XRD results in Fig. 4 indicate that the different samples mainly consist of the same phase, i.e., wollastonite ($CaSiO_3$) and hedenbergite ($CaFe(Si_2O_6)$). As shown in Fig. 5, the crystallinity was higher and the precipitation of the grains was smaller when 4wt% of Fe_2O_3 was added to the raw materials. The internal structure of the glass-ceramics was fine and close, so the density of sample ZLFe4 was the highest among the investigated samples. All of the samples exhibited a similar Mohs hardness of 7. Taking the economy of the product into account, the best sample would be the ZL specimen. However, if the material's preferred color is green, then the addition of 4wt% of Fe_2O_3 could be deemed suitable. The additional Fe_2O_3 and the Fe_2O_3 already contained in the slag together contributed to the observed crystallization behavior of the CAS system.

4. Conclusions

(1) Different amounts of Fe_2O_3 were added to naturally cooled yellow phosphorus furnace slag as a nucleating agent. The crystallization activation energy of the CAS system was found to first increase and then decrease with increasing amount of added Fe_2O_3. A white glass-ceramic with good performance was obtained when no extra Fe_2O_3 was added as a nucleating agent. With the addition of 4wt% Fe_2O_3, a gray-green glass-ceramic with good performance was obtained. This study provides a theoretical framework for the comprehensive utilization of yellow phosphorus furnace slag.

(2) Wollastonite ($CaSiO_3$) and hedenbergite ($CaFe(Si_2O_6)$) were identified as the main crystal phases in the glass-ceramics prepared from naturally cooled yellow phosphorus furnace slag. No discernible effect on the phase composition of the CAS system was observed when the dosage of Fe_2O_3 was varied.

(3) The Mohs hardness of the prepared CAS glass-ceramics containing Fe_2O_3 was 7. The samples with additional Fe_2O_3 showed stronger acid resistance and alkali resistance and lower water absorption than sample ZL. Therefore, this material (ZLFe4) could be successfully used for building decoration purposes.

Acknowledgements

This work was financially supported by the Fund for Analyzing and Testing of Kunming University of Science and Technology (Nos. 2016P2014607009 and 2016T11304019).

References

[1] Z.S. Abisheva, E.G. Bochevskaya, A.N. Zagorodnyaya, T.A. Shabanova, and Z.B. Karshigina, Technology of phosphorus slag processing for preparation of precipitated silica, *Theor. Found. Chem. Eng.*, 47(2013), No. 4, p. 428.

[2] J. Zhou, Z. Shu, X.H. Hu, and Y.X. Wang, Direct utilization of liquid slag from phosphorus-smelting furnace to prepare cast stone as decorative building material, *Constr. Build. Mater.*, 24(2010), No. 5, p. 811.

[3] J.A. Bhat, M.C. Kundu, G.C. Hazra, G.H. Santra, and B. Mandal, Rehabilitating acid soils for increasing crop productivity through low-cost liming material, *Sci. Total Environ.*, 408(2010), No. 20, p. 4346.

[4] Z. Shu, J. Zhou, Y.X. Wang, and X.S. Lu, On-site preparation of opaque glass using liquid phosphorus slag, *Earth Sci. J. China Univ. Geosci.*, 34(2009), No. 6, p. 1019.

[5] X.H. Niu, Y.C. Wang, Y.H. Jiao, B.C. Li, and G.P. Luo, Thermodynamic analysis on crystallization of glass-ceramics prepared from blast furnace slag, *Trans. Mater. Heat Treat.*, 36(2015), No. 1, p. 6.

[6] Z.H. Yang, Q. Lin, S.C. Lu, Y. He, G.D. *Liao*, and Y. Ke, Effect of CaO/SiO_2 ratio on the preparation and crystallization of glass-ceramics from copper slag, *Ceram. Int.*, 40(2014), No. 5, p. 7297.

[7] J.W. Cao and Z. Wang, Effect of Na_2O and heat-treatment on crystallization of glass-ceramics from phosphorus slag, *J. Alloys Compd.*, 557(2013) , No. 25, p. 190.

[8] Y. Zhao, D.F. Chen, Y.Y. Bi, and M.J. Long, Preparation of low cost glass-ceramics from molten blast furnace slag, *Ceram. Int.*, 38(2012), No. 3, p. 2495.

[9] L. Gan, C.X. Zhang, J.C. Zhou, and F.Q. Shangguan, Continuous cooling crystallization kinetics of a molten blast furnace slag, *J. Non Cryst. Solids*, 358(2012), No. 1, p. 20.

[10] H.Y. Liu, H.X. Lu, D.L. Chen, H.L. Wang, H.L. Xu, and R. Zhang, Preparation and properties of glass–ceramics derived from blast-furnace slag by a ceramic-sintering process, *Ceram. Int.*, 35(2009), No. 8, p. 3181.

[11] Z.H. Yang, Q. Lin, J.X. Xia, Y. He, G.D. Liao, Y. Ke, Preparation and crystallization of glass-ceramics derived from iron-rich copper slag, *J. Alloys Compd.*, 574(2013), p. 354.

[12] C.J. Liu, P.Y. Shi, D.Y. Zhang, and M.F. Jiang, Development of glass ceramics made from ferrous tailings and slag in China, *J. Iron Steel Res. Int.*, 14(2007), No. 2, p. 73.

[13] T. Toya, A. Nakamura, Y. Kameshima, A. Nakajima, and K. Okada, Glass-ceramics prepared from sludge generated by a water purification plant, *Ceram. Int.*, 33(2007), No. 4, p. 573.

[14] M. Rezvani, B. Eftekhari-Yekta, M. Solati-Hashjin, and V.K. Marghussian, Effect of Cr_2O_3, Fe_2O_3 and TiO_2 nucleants on the crystallization behaviour of SiO_2–Al_2O_3–CaO–MgO(R_2O) glass-ceramics, *Ceram. Int.*, 31(2005), No. 1, p. 75.

[15] A.A. Omar, A.W.A. El-Shennawi, and G.A. Khater, The role of Cr_2O_3, LiF and their mixtures on crystalline phase formation and microstructure in Ba, Ca, Mg aluminosilicate glass, *Br. Ceram. Trans. J.*, 90(1991), No. 6, p. 179.

[16] G.A. Khater and E.M.A. Hamzawy, Effect of different nucleation catalysts on the crystallization behaviour, within the CaO–MgO–Al_2O_3–SiO_2 system, *Silic. Indus.*, 73(2008), No. 7-8, p. 103.

[17] P. Alizadeh, B.E. Yekta, and A. Gervei, Effect of Fe_2O_3 addition on the sinterability and machinability of glass-ceramics in the system MgO–CaO–SiO_2–P_2O_5, *J. Eur. Ceram. Soc.*, 24(2004), No. 13, p. 3529.

[18] S.M. Wang, Effects of Fe on crystallization and properties of a new high infrared radiance glass-ceramics, *Environ. Sci. Technol.*, 44(2010), No. 12, p. 4816.

[19] Z.J. Wang, W. Ni, K.Q. Li, X.Y. Huang, and L.P. Zhu, Crystallization characteristics of iron-rich glass ceramics prepared from nickel slag and blast furnace slag, *Int. J. Miner. Metall. Mater.*, 18(2011), No. 4, p. 455.

[20] Z.J. Yang, Y. Li, D.Q. Cang, M.L. Diao, and W.B. Guo, The influence of Fe^{2+} and Fe^{3+} on crystallization of CaO–Al_2O_3–SiO_2–MgO system glass-ceramics, *Mater. Sci. Technol.*, 20(2012) , No. 2, p. 45.

[21] M. Avrami, Kinetics of phase change: I. General theory, *J. Chem. Phys.*, 7(1939), No. 12, p. 1103.

[22] W.A. Johnson and R.F. Mehl, Reaction kinetics in processes of nucleation and growth, *Trans. AIME.*, 135(1939), p. 369.

[23] H.E. Kissinger, Variation of peak temperature with heating rate in differential thermal analysis, *J. Res. Nat. Bur. Stand.*, 57(1956), No. 4, p. 2172.

[24] H.E. Kissinger, Reaction kinetics in differential thermal analysis, *Anal. Chem.*, 29(1957), No. 11, p. 1702.

[25] X. Z. Ren, W. Zhang, Y. Zhang, P.X. Zhang, and J.H. Liu, Effects of Fe_2O_3 content on microstructure and mechanical properties of CaO–Al_2O_3–SiO_2 system, *Trans. Nonferrous Met. Soc. China*, 25(2015), No. 1, p. 137.

[26] H.X. Li, B.W. Li, X.F. Zhang, X.L. Jia, M. Zhao, and Z.W. Zhang, Influence of Fe_2O_3 on the microstructure and properties of the nanocrystalline tailing-based glass-ceramics, *J. Synth. Cryst.*, 45(2016), No. 1, p. 176.

[27] B. Xu, J.W. Cao, and K.M. Liang, Influence of Fe_2O_3 on the crystallization and foaming of CaO–Al_2O_3–SiO_2 glass-ceramics, *Rare Met. Mater. Eng.*, 40(2011), Suppl. 1, p. 15.

[28] Z.J. Wang, W. Ni, Y. Jia, L.P. Zhu, and X.Y. Huang, Crystallization behavior of glass ceramics prepared from the mixture of nickel slag, blast furnace slag and quartz sand, *J. Non Cryst. Solids*, 356(2011), No. 31-32, p. 1554.

[29] K. Singh and D. Bahadur, Characterization of SiO_2–Na_2O–Fe_2O_3–CaO–P_2O_5–B_2O_3 glass ceramics, *J. Mater. Sci. Mater. Med.*, 10(1999), No. 8, p. 481.

[30] Y.L. Tian, *New Glass Technology*, China Light Industry Press, Beijing, 2013, p. 86.

[31] B. Li, L.H. Wen, and C. Ma, Effect of Fe_2O_3 on properties of CaO–SiO_2 glasses and glass-ceramics, *J. Ceram.*, 28(2007), No. 2, p. 99.